Available online at www.sciencedirect.com
SCIENCE DIRECT®
Chemistry and Physics of Lipids 133 (2005) 37–49
CPL
CHEMISTRY AND PHYSICS OF LIPIDS
www.elsevier.com/locate/chemphyslip

# Enzymatic lipid removal from surfaces—lipid desorption by a pH-induced "electrostatic explosion"

Torben Snabe, Maria Teresa Neves-Petersen, Steffen Bjørn Petersen*

*Department of Physics and Nanotechnology, Biostructure and Protein Engineering Group, Aalborg University, DK-9000 Aalborg, Denmark*

Received 1 August 2003; received in revised form 12 August 2004; accepted 24 August 2004
Available online 12 October 2004

**Abstract**

Removal of lipidic molecules from surfaces can be accomplished using detergents containing lipases. Surface cleaning is usually performed under alkaline conditions due to increased solubility of the hydrolysis products, especially free fatty acids. This paper shows that removal of a triacylglycerol film from a surface can be dramatically enhanced in a sequential system where pH is shifted to alkaline conditions after an initial lipolytic reaction period at or below neutral pH. Data from three different biophysical techniques, attenuated total reflection Fourier transform infrared spectroscopy (ATR-FTIR), quartz crystal microbalance with dissipation monitoring (QCM-D), and total internal reflection fluorescence spectroscopy (TIRF) clearly show the effects of such cleaning procedure. Initially the reaction is carried out at pH below the p$K_a$ value of the fatty acids formed upon triacylglycerol hydrolysis, and the protonated fatty acids accumulate in the film. The mechanism of lipid removal, induced by increasing pH to a value above the fatty acid p$K_a$, is explained by a burst caused by electrostatic repulsion between rapidly ionised fatty acids, i.e. by an "electrostatic explosion". Performing the initial hydrolysis at pH 6 and the subsequent rinse at pH 10, using triolein as model substrate, lipid removal from surfaces by both commercial detergent lipases and non-commercial lipases was significantly improved compared to a reaction at constant pH 10.


*Keywords:* Lipase activity; Lipid removal; Lipase adsorption; Triacylglycerol; ATR-FTIR; QCM-D; TIRF

## 1. Introduction

A major problem when cleaning surfaces is the removal of adsorbed lipid deposits, which often contain oily, longchained, and water-insoluble triacylglycerols. Detergent formulations usually contain lipolytic enzymes (lipases, formally triacylglycerol lipases, E.C. 3.1.1.3), which degrade triacylglycerols into free fatty acids, di- and mono-acylglycerols, and possibly glycerol. These hydrolysis components, especially the fatty acids, are more water soluble compared to triacylglycerols (Fujii et al., 1986). With aid from

* Corresponding author. Tel.: +45 96358469; fax: +45 96359129.
*E-mail address:* sp@nanobio.aau.dk (S.B. Petersen).
*URL:* http://www.nanobio.aau.dk (S.B. Petersen).

0009-3084/$ – see front matter © 2004 Elsevier Ireland Ltd. All rights reserved.
doi:10.1016/j.chemphyslip.2004.08.005

detergent components and their ability to form water soluble aggregates, fatty acids may solubilize into the aqueous washing solution and thereby be released from the surface. Lipases are essential in detergent formulations when cleaning at low temperatures (Dambmann et al., 1971).

The lipase from *Thermomyces lanuginosus*, formerly *Humicola lanuginosa*, was the first major commercial lipase for detergents. The *T. lanuginosus* lipase (TLL) is produced and sold by Novo (now Novozymes, Denmark) since 1989 as lipolase (Aaslyng et al., 1991). Though lipolase is stable in detergent formulations, at high pH, and at high temperatures, 2–3 wash cycles (which includes drying of the textile) are needed to obtain a significant removal of lipidic stains (Flipsen et al., 1998; Aaslyng et al., 1991).

One suggestion explaining this lack of "first wash activity" by lipolase is that the main lipolytic activity occurs during the drying process (Flipsen et al., 1998; Aaslyng et al., 1991). Triacylglycerol removal is therefore only achieved after the second wash when the detergent solution and the mechanical stress can remove the hydrolysis products produced during the first drying (Aaslyng et al., 1991).

We have outlined in a previous paper an alternative explanation, suggesting that the formation rate of ionised fatty acids (as a result of lipase activity) must exceed a certain threshold in order to obtain lipid removal (Snabe and Petersen, 2003). The mechanism is explained by an equilibrium between hydrolysis products being incorporated into the substrate film or forming micelle-like aggregates which can be solubilized and ejected into the aqueous solution. Interestingly, it was found that the equilibrium favours lipid removal only under alkaline and $Ca^{2+}$-free conditions and when the lipolytic rate is above a certain threshold. Consequently it was proposed that the equilibrium of lipid removal is controlled by the formation rate of ionised fatty acids.

Flipsen et al. (1998) reported an empirical study of the removal of triolein soil from textile using lipases. It was found that the triacylglycerol lipase cutinase displayed significant lipid removal (20%) at constant pH 9—thus cutinase can be termed a "first-wash lipase". However, in a sequential system where the initial incubation at pH 9 was followed by a subsequent wash at pH 10.5–11, the removal of lipid increased to 35%. The improvement was explained in terms of increasing lipid solubility in aqueous environment at increasing pH values.

The present paper shows that significant lipid removal from surfaces by a large range of lipases can be induced by carrying out the washing procedure at two different pH values. The washing process is preferably started below the p$K_a$ value of the released fatty acids. Hydrolysis should then be allowed to progress for some time allowing accumulation of protonated fatty acids in the lipid film. Subsequently the pH of the solution in contact with the surface to be cleaned is raised above the p$K_a$ value of the fatty acid molecules. This procedure results in a significantly improved lipid removal (up to 50%) compared to the usual procedure performed under constant alkaline conditions. Using the longchained triolein as substrate, results are presented with the native *T. lanuginosus* lipase (TLL) and engineered TLL variants, as well as lipases from *Rhizomucor miehei*, *Pseudomonas cepacia*, and *Fusarium solani* pisi (cutinase).

## 2. Materials and methods

### 2.1. Materials

Triolein 99% (Fluka 92859, lot. 2045347) was used as substrate. Seven triacylglycerol lipases (E.C.3.1.1.3) were used: *T. lanuginosa* lipase (TLL) and engineered TLL variants, i.e. lipolase, lipoprime, lipex, and an inactive TLL (Novozymes, Denmark), as well as lipases from *R. miehei* (Sigma L9031, lot 32K2604) *Ps. cepacia* (Sigma L9156, lot 85H2604), and *F. solani* pisi (cutinase) produced in our laboratory (Petersen et al., 1998). Protein concentrations were determined using $UV_{280}$ absorption and the respective extinction coefficients at 280 nm. Buffer of $3\times$ 25 mM citrate–Tris–glycine (25 mM of each component) with or without 10 mM $CaCl_2$ was prepared from citrate trisodium dihydrate 99% (Sigma S4641,19H0717), glycine 99.5% (Acros Organics, 220910010/200-272-2), Tris 99.9% (Applichem A1086,C2101), and calcium chloride dihydrate 99.5% (Merck 1.02382, lot TA401282). pH was adjusted with 3 M sodium hydroxide or hydrochloric acid and filtered through a 0.20 μm filter before use (Sartorius Minisart 16534 K). Reagents for preparation and triolein coating of TIRF quartz slide surfaces: dichlorodimethylsilane (Fluka 40150,

lot 413248/1), trichloroethylene (Aldrich 13,312-4, lot U00885), 1% (v/v) triolein in *n*-hexane (Merck 1.04367 lot I1020367-142). Reagents for preparation of gold QCM-D crystal surfaces: octadecylmercaptan 98% (Sigma O185-8, lot 17625-0201) in *n*-hexane. For oleic acid film titration, oleic acid (Sigma O1630, lot 48H5218) was used.

### 2.2. Methods

Lipolysis of a triolein film on a hard surface support was analyzed. ATR-FTIR and QCM-D was used for chemical and physical analysis of the lipid film, while TIRF was used for monitoring lipase adsorption to the film. All experiments were performed at 25 °C (±0.5 °C).

#### 2.2.1. ATR-FTIR analysis of the remaining film after hydrolysis

Chemical analysis of the remaining lipid film after the lipolytic reaction was performed using attenuated total reflection infrared spectroscopy (ATR-FTIR).

*2.2.1.1. ATR-FTIR Instrumental.* A Bruker IFS 66V/S FTIR spectrometer with a deuterium triglycine sulphate (DTGS) detector was used (purchased from Bruker Optics, Germany). The sampling unit was a 1 cm × 7 cm large 45° ZnSe attenuated total reflectance (ATR) crystal with six internal reflections at the crystal–sample interface. The ATR crystal made out the base in a reaction chamber of height ∼0.1 cm and a total volume of ∼1.1 ml (Fig. 1). A continuous flow through the chamber was applied using a peristaltic pump. Each spectrum was averaged from 32 scans recorded at a scan rate of 10 kHz at a resolution of 4 $cm^{-1}$. Data was collected in the 4000–800 $cm^{-1}$ range. The general theory and applications of the ATR-FTIR technique have been covered in sufficient depth elsewhere (Harrick, 1967; Griffiths and de Haseth, 1986) and is therefore not described further in the present paper. Specifically for triacylglycerol film analysis we refer to Snabe and Petersen (2002, 2003).

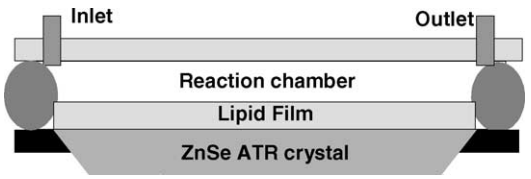


Fig. 1. Set-up of the ATR-FTIR flow reaction chamber, with the ZnSe ATR crystal as base, a rubber O-ring as spacer wall, and a plexiglass plate as lid. The incident infrared radiation angle was 45° and six internal reflections were introduced to the active surface (towards the reaction chamber). The volume of the reaction chamber was approximately 1.1 ml, created by a height of 0.1 cm and a total base area of 11 $cm^2$ (of which 7 $cm^2$ was the ATR crystal and the remainder was the surrounding teflon-coated crystal holder). Note that dimensions are not in correct proportions.

*2.2.1.2. ATR-FTIR experimental.* Experiments were performed using the following procedure: A thin film of pure triolein was carefully applied by distributing a drop uniformly on the hydrophobic ZnSe ATR crystal surface with a cotton stick until the absorbance for the carbonyl ester peak (1745 $cm^{-1}$) was 0.28–0.32 absorbance units. After mounting the lid, the water insoluble triolein film was exposed to buffer at pH 6 or 10 for 10 min (a volume of 5 ml buffer circulated through the reaction chamber using a peristaltic pump at a constant flow rate of 3.5 ml $min^{-1}$). Then hydrolysis was initiated by circulating a fresh buffer solution at pH 6 or 10 with lipase through the reaction chamber for 20 min. After 20 min, fresh "rinsing buffer" at pH 10 was circulated in the system for 10 min. Subsequently, the reaction chamber was drained before the film was exposed to a buffer at pH 10 with 10 mM $Ca^{2+}$ for 2 min. Finally, the chamber was drained again and the film was allowed to air dry before an infrared spectrum of the remaining lipid film was recorded.

The relative content of total lipid remains on the ATR crystal were analyzed by simple absorption spectrum integration of the hydrocarbon region at 3050–2700 $cm^{-1}$ (mainly $CH_2$ and $CH_3$–vibrations). The presence of fatty acid products in the film were identified in the region at 1600–1520 $cm^{-1}$ (fatty acid carbonyl vibrations in complex with $Ca^{2+}$). Lipids in the reaction buffer (at pH 6 or 10) and the rinsing buffer (at pH 10) were extracted by mixing thoroughly with 25% *n*-hexane. The extracted lipids were analyzed qualitatively by applying 10–20 μl of the hexane phase on the ATR crystal surface. After evaporation of the hexane an infrared spectrum of the extracted lipids was recorded. After each measurement, the ATR crystal surface was cleaned carefully using ethanol and lens paper.

*2.2.2. ATR-FTIR analysis of oleic acid ionisation*

In order to observe the ionisation state of oleic acid as a function of pH, a thin film of pure oleic acid was applied on the ATR crystal and exposed to buffers ranging from pH 5–10. After 5–10 min of incubation with buffer the sample spectrum (oleic acid with buffer) was recorded using the pure buffer spectrum as background. The resulting spectra were normalised against the $CH_2$–peak at $\sim$1465 $cm^{-1}$ in order to improve the visualisation.

*2.2.3. QCM-D analysis of the lipid film during hydrolysis*

Quartz crystal microbalance with dissipation monitoring (QCM-D) was applied for lipid film characterisation (film thickness and viscoelastic properties) during lipolytic degradation.

*2.2.3.1. QCM-D instrumental.* QCM-D is a state-of-the-art technique for surface analysis in liquid media. The technique is based on the oscillation of a piezoelectric quartz crystal dish where the oscillation frequency (*F*) and the oscillation energy dissipation (*D*) characterises the mass and the viscoelastic properties of the molecules adsorbed on the crystal surface. Adsorption of biomolecules to surfaces and viscoelastic characterisation of polymer films are among the usual applications. The technique for the current purpose—characterisation of a triolein film during enzymatic degradation—has recently been described in detail (Snabe and Petersen, 2003). Among other relevant references to the QCM-D technique the authors refer to Rodahl et al. (1997), Höök et al. (1999, 2001), Voinova et al. (1999).

A quartz crystal microbalance and dissipation device (Q-Sense D301) purchased from Q-Sense AB (Göteborg, Sweden) and a gold-coated piezoelectric quartz crystal with a fundamental frequency of 5 MHz was used. The active gold surface of the 14 mm large quartz crystal (diameter) formed the base in a reaction chamber with a volume of $\sim$80 μl (height $\sim$ 0.5 mm) in which a rapid exchange of reaction liquid was possible (Fig. 2).

*2.2.3.2. Surface preparation and triolein film coating of the QCM-D crystal surface.* The gold surface on the QCM-crystal is hydrophilic. In order to achieve a hydrophobic surface, a monomolecular alkane

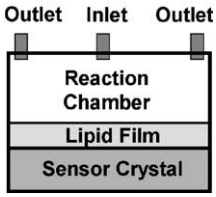


Fig. 2. The QCM-D set-up with the piezoelectric quartz crystal sensor as base in the reaction chamber. The sensor surface is circular with a diameter of 14 mm and the chamber height is $\sim$0.5 mm, i.e. the chamber volume is $\sim$80 μl. Note that dimensions are not in correct proportions in this illustration.

(octadecyl) film with a terminal thiol group (–SH) was covalently bound to the gold surface. Before preparing the surface, a thorough cleaning process was conducted, where the crystal first was illuminated with UV-light for 30 min, then immersed into a solution of 1:1:5 of $H_2O_2$:$NH_3$:deionised $H_2O$ at 75 °C for 5 min, and subsequently rinsed thoroughly with deionised water. The crystal was then immersed into a solution of 1 mM octadecylmercaptan ($HS(CH_2)_{17}CH_3$) in *n*-hexane for at least 2 h at ambient room temperature (20–25 °C), rinsed in pure *n*-hexane, ethanol, and deionised water, and finally dried with nitrogen gas.

*2.2.3.3. QCM-D experimental.* A triolein film was prepared manually by carefully distributing a drop of pure triolein on the hydrophobic QCM-D quartz crystal surface using a piece of soft lens paper. The shift of the fundamental frequency was within 250–500 Hz. Before applying the enzyme, the film was hydrated in the buffer (pH 6 or 10) for 8 min upon adding fresh buffer three times. Every buffer addition was performed by entering 0.5 ml through the reaction chamber, ensuring thorough exchange of the liquid in the reaction chamber (flow was controlled by gravity—buffer exchange lasted 3–5 s). Enzyme addition was performed also by letting 0.5 ml lipase solution (2 μg $ml^{-1}$) in the same buffer stream through the measurement chamber. After 20 min hydrolysis, 0.5 ml buffer at pH 10 was applied.

The frequency (*F*) and dissipation (*D*) were obtained for the fundamental frequency, the 3rd, and the 5th overtone (i.e. 5, 15, and 25 MHz) and modeled using the viscoelastic model based on the Voight representation (software: Q-Tools, Q-Sense AB, Göteborg). The viscoelastic model is applicable for polymeric films with predominantly liquid characteristics and provides

modeled values of the film thickness ($d_f$), viscosity ($\eta_f$), and elasticity ($\mu_f$). Model details are described elsewhere (Voinova et al., 1999; Höök et al., 2001; Snabe and Petersen, 2003). Model constants were the solvent density ($\rho_l = 10^3\,kg\,m^{-3}$), the solvent viscosity ($\eta_l = 10^{-3}\,kg\,m^{-1}\,s^{-1}$), and the film density ($\rho_f = 0.95{\cdot}10^3\,kg\,m^{-3}$). Initial values for the variable film parameters were: $\eta_f = 4\,kg\,m^{-1}\,s^{-1}$; $\mu_f = 1.5 \times 10^5$ Pa; $d_f = 100$ nm.

After each measurement, the system was cleaned with helmanex (non-ionic detergent), 99% ethanol, and deionised water, and subsequently dried with nitrogen gas. A sufficient surface hydrophobicity was verified by visually controlling that the contact angle of a water drop on the crystal surface was more than 90°.

### 2.2.4. TIRF measurements

Total internal reflection fluorescence (TIRF) spectroscopy was used in order to monitor lipase adsorption and desorption from a hydrophobic surface coated with triolein.

*2.2.4.1. TIRF instrumental.* TIRF employs the phenomenon of total internal reflection of an electromagnetic wave that occurs at the interface between two transparent media with different refractive indices when the incident angle is greater than the critical angle. In brief, when a beam of light propagating within a medium of higher refractive index ($n_1$) (e.g. quartz) encounters an interface with a medium of lower refractive index ($n_2$) (e.g. water) the light undergoes total internal reflection if the incident angles ($\theta_i$) is greater than the critical angle ($\theta_c$). The critical angle is defined as $\theta_c = \sin^{-1}(n_1/n_2)$. Interference of the incident and reflected beams generates a standing electromagnetic wave with maximum amplitude of the electric vector at the interface. An exponentially decaying electromagnetic wave, the evanescent wave, penetrates into the less condensed medium (i.e. the aqueous solution), while the main part of the incident light is reflected back into optically more condensed medium of quartz. The penetration depth ($d_p$) of the evanescent wave into the sample medium is a function of the incidence angle, the refractive index ratio, and the incident light wavelength ($\lambda_i$):

$$d_p = \lambda_i[(2\pi n_1)(\sin^2(\theta_i) - (n_2/n_1)^2)^{0.5}]^{-1}.$$

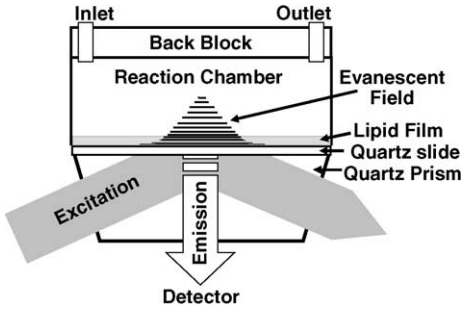


Fig. 3. Illustration of the TIRF flow cell. The volume of the reaction chamber is approximately 3.5 μl, created by a height of 0.01 mm and a base area of approximately 350 $mm^2$ (a rectangular shape of 16 mm broad and 24 mm long with cut edges). Note that dimensions are not in correct proportions.

In the current system the penetration depth of the evanescent field is in the order of 112 nm ($\theta_i \approx 72°$; $\lambda_i = 280$ nm; $n_{quartz} = 1.46$ and $n_{water} = 1.33$). Thus, the evanescent wave provides surface selectivity to TIRF and allows measurements of surface concentration of fluorescent adsorbed molecules, e.g. proteins.

A TIRF system (BioElectroSpec Inc., Harrisburg, PA) coupled with a fluorescence spectrophotometer (PTI QM-2000 from Photon Technology Int., Lawrenceville, NJ) with a 75 W Xenon arc source was used. The PTI instrument excitation and emission slits were set to 6 nm. The sample in the flow chamber was excited at 280 nm and the fluorescence emission intensity was monitored at 330 nm. The flow chamber was comprised by a "sandwich" consisting of a TIRF quartz prism, a TIRF quartz slide (with the sample surface), a 10-μm gasket (comprising the chamber thickness), and a back block with holes to channel the solution through the flow chamber (Fig. 3). The dimension of the flow chamber is 16 mm × 24 mm × 0.01 mm (3.8 μl). The excitation light travels through the prism and slide, hits the interface between slide and solution, and totally internally reflects from the interface back into the slide and prism. The reflected beam generates an evanescent electromagnetic field in the middle of the TIRF slide. This area of the TIRF slide serves thus as the sensor surface. Only fluorophores that are present at the surface and in close proximity of the surface (within the evanescent field) are excited and fluoresce.

*2.2.4.2. Surface preparation and triolein film coating of the TIRF quartz slide.* Chemical modification of

glass, quartz and metal oxide surfaces involves silanization. Silane chemistry allows functionalisation of a quartz surface with different active groups, such as methyl groups. In order to prepare a hydrophobic surface for TIRF measurements (in order to improve lipid adhesion), the quartz slide was methylated by incubating the surface with 0.3% (v/v) dichlorodimethylsilane in trichloroethylene for 30 min at ambient room temperature (20–25 °C). Subsequently, the surface was rinsed in pure trichloroethylene for 5 min and finally flushed thoroughly with ethanol and deionised water before drying with nitrogen gas. The methylation procedure was based on a procedure described by Buijs and Hlady (1997). The methylated slide was then attached on the TIRF quartz prism using glycerol in between them (glycerol and quartz have almost equal refractive indices and let the light pass with minimal interference). The triolein film was prepared by distributing 20 μl triolein–hexane solution (0.1%, v/v) on the methylated surface using the side of a pipette tip. After hexane evaporation, the triolein film appeared as a homogeneous "foggy" film on the surface.

*2.2.4.3. TIRF experimental.* The TIRF flow-chamber was prepared by placing the gasket between the triolein coated slide/prism and the back block and mounted vertically in the instrument. Buffer with and without lipase was purged through the chamber at a flow rate of 0.25 ml $min^{-1}$. Experiments were performed by an initial hydration in buffer without lipase for approximately 5 min before adding 2 μg $ml^{-1}$ lipase in the same buffer (at pH 6 or 10). After 10–15 min the system was rinsed in buffer without lipase at pH 10. Fluorescence emission intensity at 330 nm (from excitation of aromatic protein residues at 280 nm) was monitored continuously during experiments (one measurement per second). After each experiment the surface was cleaned carefully with ethanol and deionised water and dried with nitrogen gas. The same surface was usable 20–30 times. A sufficient surface hydrophobicity was verified visually by controlling that the contact angle of a water drop on the crystal surface was more than 90°.

## 3. Results

The hydrolysis of a triacylglycerol film was monitored in two different pH systems. In the first system the reaction was performed under constant alkaline conditions at pH 10 (called the pH 10 system), and in the second system the reaction was carried out at pH 6 followed by a rinse at pH 10 (called the pH 6–10 system).

### *3.1. Chemical film analysis (ATR-FTIR)*

Based on integration of the hydrocarbon peaks at 3050–2700 $cm^{-1}$ in the infrared spectra of the remaining dry film after the reactions, the relative levels of total lipid (both hydrolysed and non-hydrolysed) were computed (Fig. 4). It is observed that removal of lipid molecules is enhanced in the pH 6–10 system compared to the pH 10 system. This is true for all the lipases tested—except for lipoprime where the level of the remaining lipid film is equally low in both systems. Lipolase was tested at two concentrations (2 and 10 μg $ml^{-1}$). In the pH 6–10 system a concentration effect on lipid removal was observed, i.e. using 10 μg $ml^{-1}$ lipolase results in the largest lipid removal, while no concentration effect was found in the pH 10 system. The control experiments without protein show an equal high level of remaining lipid in the pH 10 and 6–10 system.

In addition, for all lipases it was observed visually that lipidic bodies were released immediately from the surface when pH was shifted to pH 10 after the initial reaction at pH 6 (observed by looking into the reaction chamber through the transparent chamber lid when pH was shifted).

A qualitative activity control was carried out by detecting if free fatty acids had been formed and were present on the film after the reaction. When no lipase was added, no fatty acids were detected in either pH system, while for all lipases tested fatty acids were detected in both pH-systems, showing that lipolytic activity had occurred (data not shown).

Analysis of the supernatant in the pH 10 system showed that only fatty acids and no ester molecules were released into the aqueous phase (in this reaction ester containing molecules can be monoolein, diolein, and triolein). It is important to note that in the pH 6–10 system both fatty acids and ester molecules were released into the aqueous solution when shifting from pH 6 to 10 (data not shown).

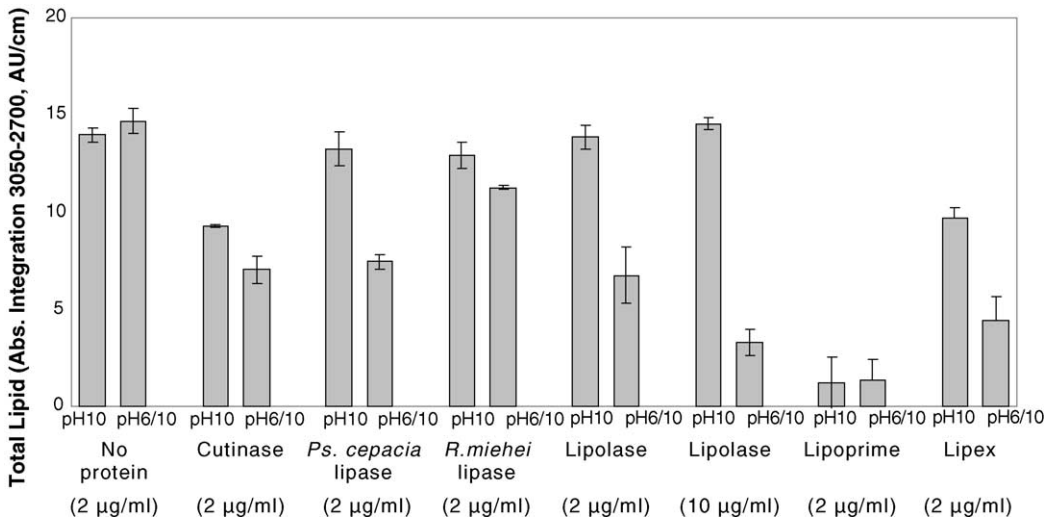


Fig. 4. Signal from lipid acyl chains in remaining dry film after reaction (total lipid content, i.e. both substrate and hydrolysis products). The values were determined by integration of the peaks in the hydrocarbon region at 3050–2700 $cm^{-1}$ (ATR-FTIR measurements).

### 3.2. Physical film analysis (QCM-D)

QCM-D measurements were performed using lipolase. The raw data (*F* and *D*) were similar to the data obtained previously also at pH 10 without $Ca^{2+}$ (Snabe and Petersen, 2003). Raw data were computed with the viscoelastic model which provided the modeled values of the thickness and the viscoelastic properties (viscosity and elasticity) of the film during the reaction (Fig. 5).

Under constant alkaline conditions (pH 10, Fig. 5a), no or minor thickness decrease was observed during the 20 min of hydrolysis ($t$ = 7–27 min), while both the viscosity and elasticity decreased significantly (to 60–70% and 20–40% of the initial values, respectively). The rinse with buffer at pH 10 ($t$ = 27 min) induced no significant changes in any of the measured parameters.

During 20 min of hydrolysis ($t$ = 7–27 min) at pH 6 (Fig. 5b), there was no or minor changes in the film thickness, and the film viscosity and the elasticity decreased with a similar rate as during the initial hydration ($t$ = 0–7 min). The rinse at pH 6 ($t$ = 27 min) induced no significant changes, while the following rinse at pH 10 ($t$ = 29 min) induced a rapid decrease in thickness, viscosity, and elasticity. The film thickness decreased to 30–50% of its initial thickness, the film viscosity decreased to 50–60% of its initial value, and the elasticity to 10–20% of its initial value.

### 3.3. Lipase adsorption (TIRF)

Lipase adsorption experiments on a triolein-coated surface monitored by TIRF are exemplified with cutinase and lipoprime (Fig. 6). The protein fluorescence emission intensity signal at 330 nm stemming from proteins at or close to the surface (within the evanescent field) is correlated to the level of lipase adsorbed on the film during hydrolysis. It can be observed in Fig. 6 that the fluorescence emission increases almost linearly when proteins enter the TIRF reaction chamber and start adsorbing to the surface. After 5–10 min maximum emission intensity is observed followed by a decrease in fluorescence emission intensity.

Adsorption data for cutinase (Fig. 6a)—which were qualitatively representative also for *R. miehei*, *Ps. cepacia*, and native TLL (lipolase)—show that lipase adsorption is very low in the constant pH 10 system. In the pH 6–10 system adsorption is high during the initial reaction at pH 6, while the shift from pH 6 to 10 induces desorption of protein from the surface. Lipoprime and lipex also display the largest adsorption at pH 6 compared to pH 10, and desorption is observed in the pH 6–10 system when rinsing at pH 10 as well (exemplified with lipoprime, Fig. 6b). Lipoprime and lipex (which are TLL variants engineered for enhanced adsorption to lipidic surfaces) show larger adsorption both at pH 6

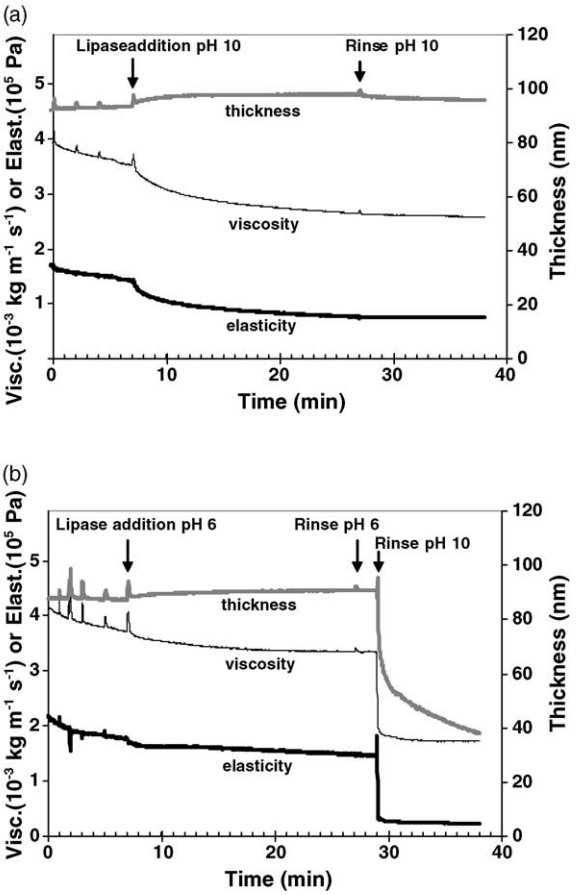


Fig. 5. QCM-D analysis of a triolein film during lipolysis using 2 μg ml$^{-1}$ Lipolase in the pH 10 system (a) and in the pH 6–10 system (b). Each plot shows the modeled film viscosity (thin black line), elasticity (thick black line), and thickness (thick grey line) during the reaction. The curves are computed from QCM-D raw data using the viscoelastic model as described. The small spikes are due to pressure changes when the solution in the chamber is applied, i.e. during hydration in buffer ($t$ = 0–7 min), upon lipase addition (at $t$ = 7 min), and when rinsing with buffer (from $t$ = 27 min).

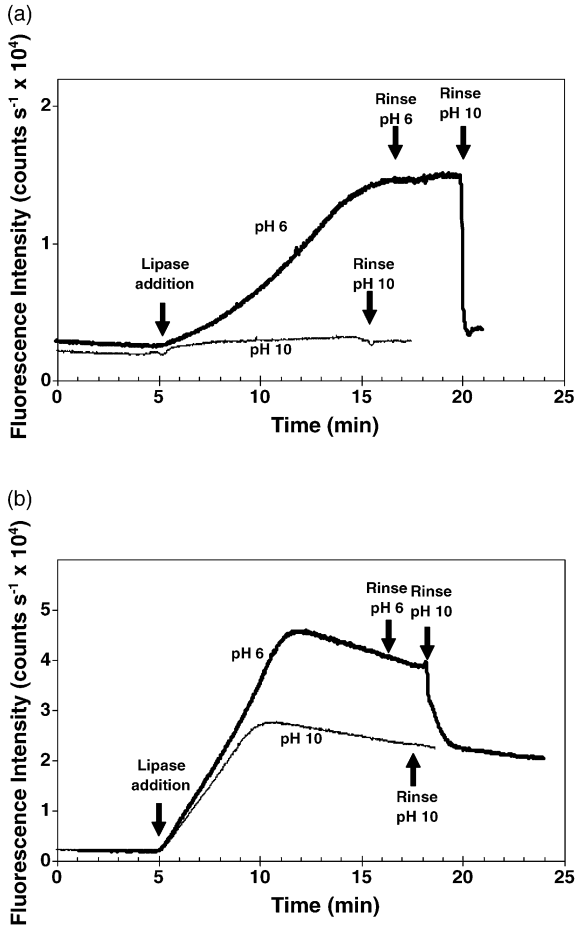


Fig. 6. Lipase adsorption of cutinase (a) and lipoprime (b) during triolein film hydrolysis at constant pH 10 (thin lines) and at pH 6–10 (thick lines). The signal is the emitted fluorescence intensity at 330 nm due to excitation at 280 nm, which signifies the amount of protein adsorbed (TIRF measurements).

and 10 compared to the other lipases. Fig. 7 shows the adsorption levels of native TLL and TLL-variants at pH 6 and pH 10, based on the maximum fluorescence emission intensity reached after 5–10 min after protein addition. Note that all experiments were carried out in buffer without $Ca^{2+}$, except one performed at pH 10 with $Ca^{2+}$ (Fig. 7 "Native pH 10 with $Ca^{2+}$").

In addition, it was observed visually that the surface after reactions using the pH 6–10 system was much cleaner compared to the reactions in the constant pH 10 system.

### 3.4. Oleic acid titration

The pH titration of a pure oleic acid film, monitored by ATR-FTIR, is shown in Fig. 8. At 1710 cm$^{-1}$ in the infrared spectrum, the carbonyl vibration of protonated free fatty acids appears, while the carbonyl vibration of ionised free fatty acids appears around 1550 cm$^{-1}$. The figure shows that the major shift occurs between pH 7 and 8, and consequently p$K_a$ of oleic acid in such a film is between 7 and 8.

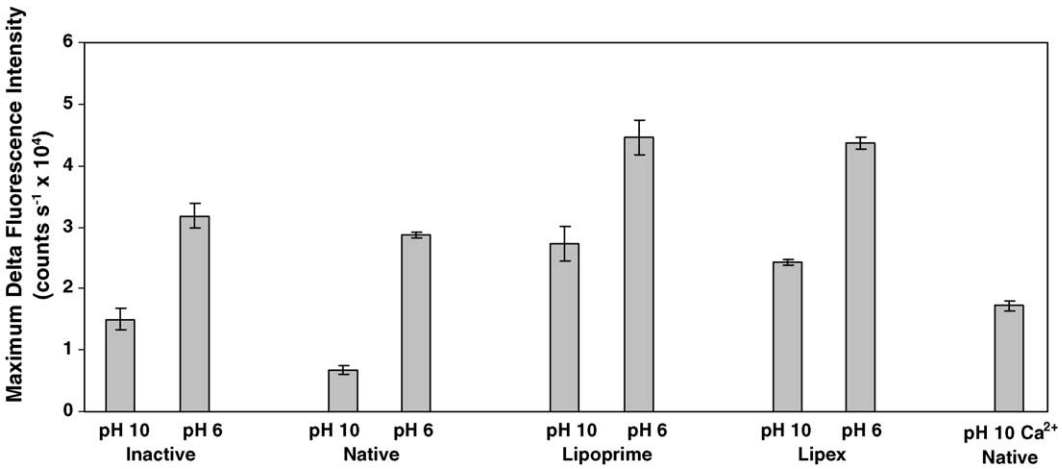


Fig. 7. Adsorption of native TLL and variants on triolein at pH 10 and 6, measured by TIRF. All experiments were performed in buffer without $Ca^{2+}$, except one experiment at pH 10 with 10 mM $Ca^{2+}$ using native TLL (right bar).

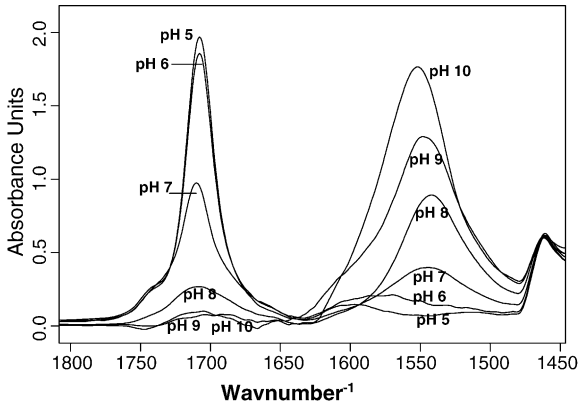


Fig. 8. Infrared spectra of an Oleic Acid film exposed to an aqueous solution in the pH 5–10 range, recorded with the pure aqueous solution as background. The infrared band for protonated oleic acid appears at ∼1710 $cm^{-1}$ and for ionised oleic acid at ∼1550 $cm^{-1}$.

## 4. Discussion

The present results show that lipase aided removal of a triacylglycerol film from a surface can be highly enhanced if lipolysis is performed at a pH below the p$K_a$ value of the released fatty acid (usually at or below pH neutral), before rinsing at a pH value above the fatty acid p$K_a$. This procedure triggers rapid removal of the lipid film present on the surface to be cleaned.

The physical state of the lipidic phase is highly complex. Aside from the intrinsic triacylglycerol molecules, it contains triacylglycerol hydrolysis products, i.e. lysoacylglycerols and fatty acids (FA). Protonated and uncharged FA molecules tends to accumulate in the film and could conveniently dissolve into the deeper lipidic layers (Snabe and Petersen, 2003). It is plausible that protonated and uncharged FA to some extent aggregate into FA conglomerates. A sudden change in pH where FA goes from a protonated (uncharged) to a deprotonated (charged) form renders the FA molecules more hydrophilic, and simultaneously each charged FA molecule will electrostatically repulse other charged FA molecules. This is likely to disrupt the FA conglomerates considering the very energetic strength of electrostatic interaction.

### 4.1. The observations of lipid removal

In terms of lipid removal, results obtained by ATR-FTIR, QCM-D, and TIRF all confirmed that hydrolysis at pH 6 followed by a shift to pH 10 proved superior to a hydrolysis performed only at pH 10:

- ATR-FTIR data show for all active lipases a significantly improved removal of lipid from the surface using the pH 6–10 system compared to the pH 10 system (Fig. 4).
- QCM-D data show that the film thickness using Lipolase is not reduced during hydrolysis at constant pH 10, while a shift from pH 6 to 10 after initial hydrolysis at pH 6 induces removal of lipid (displayed

by an immediate decrease in thickness as observed in Fig. 5b).

- Visually observed the TIRF slide surface appeared much cleaner after reactions using the pH 6–10 system compared to the pH 10 system. In addition TIRF data show that a shift to pH 10 after hydrolysis at pH 6 induces lipase desorption (Fig. 6). This can partially be explained by a secondary effect of lipid desorption, i.e. when lipase molecules are adsorbed to desorbed lipids they may be transported out of the film with the desorbing lipid (more details on lipase adsorption/desorption is outlined later).

### 4.2. The molecular mechanisms of lipid removal

Since the initial lipolysis at pH 6 of the triacylglycerol film is performed 1–2 pH units below the effective p$K_a$ of the liberated FA molecules, the FA's are protonated and uncharged, and therefore they can accumulate closely packed within the film. A subsequent pH shift from, e.g. pH 6 to 10 triggers that these closely spaced FA molecules become negatively charged and repulse one another. Accompanied by the improved water solubility of deprotonated FA as compared to protonated FA, the space induced by acid–acid repulsion favours water penetration into the film. The sudden pH shift from pH 6 to 10 causes an abrupt formation of deprotonated FA's. A high formation rate of ionised free fatty acids is necessary for efficient removal of a lipidic film, because this leads to a rapid and violent water penetration into the film. This is observed in the QCM-D experiments by a decreasing film viscosity and elasticity (Fig. 5) indicating a more loose film (detailed interpretation of QCM-D data concerning triacylglycerol film hydrolysis is described elsewhere (Snabe and Petersen, 2003)).

Rapid water penetration into the film has been suggested physically to cause the release of lipidic bodies from a lipidic film (Snabe and Petersen, 2003). In this previous study, it was shown that under constant alkaline conditions (pH 10) only high lipase activity could lead to significant removal of lipid from the surface. Low activity resulted only in swelling of the film, i.e. slow water penetration into the film, and no lipid removal. The interpretation is that a certain force, caused mainly from the rate of swelling (the rate of water penetration into the film), is required for lipid removal to occur. The same study also presented experiments performed at pH 10 with $Ca^{2+}$ and at pH 7. Under these conditions where the FA's produced appears predominantly uncharged (partially protonated at pH 7 or neutralised in complex with calcium ions at pH 10) no lipid removal was obtained. The interpretation is therefore that lipid removal requires a certain formation rate of ionised FA (Snabe and Petersen, 2003).

In the present results, a sufficient high formation rate of ionised FA for lipid removal is induced by the sudden pH shift from pH 6 to 10, and not by a high lipase activity. While only cutinase, lipoprime, and lipex display sufficient activity for lipid removal in the pH 10 system, all lipases demonstrate lipid removal in the pH 6–10 system (Fig. 4). The accumulation of protonated FA molecules in the film during the initial hydrolysis at pH 6 is essentially a build-up of potential charges, which are "activated" into the ionised form when pH is raised. The formation rate of ionised FA molecules then predominantly depends on the ionisation rate of the already accumulated FA molecules—which is many-folds larger that the lipolysis turnover. Consequently, these results strongly indicate that lipid removal using any enzyme with lipolytic activity may be improved if the cleaning procedure is designed with the described pH shift. This includes low-active lipases as well as already commercial lipases used in cleaning processes (as shown with the commercial TLL lipases). Further, lipid removal in non-enzymatic systems may also be improved, e.g. chemical hydrolysis of triacylglycerols, where the initial reaction and subsequent reaction pH values are chosen according to the p$K_a$ value of the fatty acid processed as described.

The choice of pH values are not limited to pH 6 and 10. The important parameter is that the pH shift must result in a certain amount of deprotonation of the FA molecules accumulated in the film. A system with initial activity at pH 6 and a subsequent shift to pH 8 has also shown to result in removal of lipid from the film, while activity performed only at pH 8 displayed no or minimal lipid removal (data not shown). A similar effect has been observed in a system with initial activity at pH 8 a subsequent shift to pH 10 (data not shown). In the experiments presented in this paper, a pure triacylglycerol (triolein) was utilised from which fatty acids (oleic acid) are hydrolysed. The p$K_a$ of oleic acid in a pure oleic acid film is around 7.5 (Fig. 8), and in theory oleic acid is thus fully protonated below pH 6 and fully deprotonated above pH 9. In this pH interval, the frac-

tion of protonated oleic acid molecules decreases with increasing pH. Thus, being familiar with the effective p$K_a$ value of the FA's produced during hydrolysis in a particular process, the initial activity must just be performed at a pH around or below this p$K_a$ value, and the subsequent shift must be to a pH value around or above this p$K_a$ value. However, the effect observed by a shift from pH 9 to 10.5 (as addressed in the introduction with reference to Flipsen et al., 1998) shows clearly that other pH systems may lead to similar results. Flipsen and co-workers addressed increased solubility of lipids at the higher pH as the main reason for the observed effect.

Optimisation of a triacylglycerol removal process must include considerations of both the p$K_a$ value of the free fatty acids involved and the activity optimum of the lipase (in addition to detergent formulations, which is not included in this study). In addition to the removal of a partially degraded triacylglycerol film, a similar electrostatic repulsion mechanisms could occur in a protein film under proteolytic degradation. Especially at alkaline pH when the terminal amino group and the side chains of histidine, lysine, and arginine loose their positive charges (p$K_a$ values ranging from 6–12), then there is basis for electrostatic repulsion between the negatively charged groups of the terminal carboxyl, aspartic- and glutamic acid, cysteine, and tyrosine (p$K_a$ values ranging from 4–10).

### *4.3. Electrostatics of lipase adsorption and desorption—the impact of fatty acid ionisation modulated by pH and $Ca^{2+}$*

It is shown that lipase adsorption to the lipid film at pH 6 and at pH 10 with $Ca^{2+}$ is significantly higher than at pH 10 without $Ca^{2+}$ (Fig. 7). This we explain with electrostatics, i.e. at pH 10 without $Ca^{2+}$, repulsive electrostatic forces between the film and the protein are larger than at pH 6 and at pH 10 with $Ca^{2+}$. At pH 10 without $Ca^{2+}$, repulsion may occur between negative charges of the deprotonated FA molecules accumulated in the film and vast surface regions of the lipase molecule with a negative potential. At pH 10 with $Ca^{2+}$ the FA charges appear neutralised in complex with calcium ions, and consequently the repulsive electrostatic forces are reduced. At pH 6, possible repulsive forces are also reduced because the FA molecules are protonated and appear uncharged.

In Fig. 7, it can also be observed that adsorption of the inactive TLL at pH 6 is approximately 2-fold higher than at pH 10. This is interesting because using an inactive lipase no FA molecules are produced that could lead to electrostatic repulsion between the protein and the lipid surface. However, it is known that even an uncharged oil–water interface possesses a negative potential, and that this potential becomes more negative with increasing pH (Marinova et al., 1996). Thus, because lipases also have a strong negative surface potential at pH 10—and distinctly more negative than at pH 6—adsorption is more favourable at pH 6 than at pH 10 also for the inactive lipase.

When shifting to pH 10 after some period of hydrolysis at pH 6, the general picture is that the fluorescence emission intensity drops dramatically (Fig. 6). This is partially caused by the afore-mentioned electrostatic repulsion between the proteins' surface that carries negative electrostatic potential and the negative electrostatic potential at the lipid layer. Electrostatic computations done for the lipase/esterase family of enzymes has revealed that the titration of the particular subset of residues located in and nearby the active site and binding regions of these enzymes are largely responsible for the afore-mentioned negative potential carried by the proteins' surface (Fojan et al., 2000; Neves-Petersen et al., 2001a,b; Neves-Petersen and Petersen, 2003). Furthermore, as shown with ATR-FTIR and QCM-D, a result of the pH shift is that lipid is removed from the surface. This means that the lipase molecules adsorbed onto lipid aggregates removed from the surface are also desorbed from the quartz surface and transferred away from the vicinity of the evanescent field, and consequently the fluorescence signal drops. Thus, lipase desorption is presumably a combined effect of both electrostatic repulsion between the lipase and the lipid layer and indirect desorption due to lipid removal.

In the TIRF experiments, maximum fluorescence emission intensity is reached typically after 5–10 min, and subsequently a decreasing intensity is obtained. Control experiments where the excitation beam was shut off for a few minutes showed that the emission intensity did not decrease during this period of time (data not shown). This indicates that the excited amino acids (i.e. mainly tyrosines and tryptophans) in the adsorbed lipase molecules probably are "photobleached". The fluorescence emission is thereby a sum of both adsorption and photobleaching. In addition is the level of

emission intensity influenced by the actual number of excitable amino acids at 280 nm and their position in the protein 3D-structure (due to possible effects from intermolecular shielding and quenching). The native TLL and TLL variants compared quantitatively (Fig. 7) have an identical population of tyrosines and tryptophans (Kim Borch, Novozymes, personal communication), and have therefore presumably equal characteristics in the presented fluorescence experiments.

### 4.4. Physical states and ionisation of fatty acids

Pending on the acyl chain length, the degree of saturation, temperature, metal ions present, and solvent pH, fatty acids appear in various physical states (Small, 1986; Cistola et al., 1988). Long-chained triacylglycerols may appear in an oily, homogeneous phase when protonated ($pH < pK_a$), in a laminar phase when $pH \sim pK_a$, and as water dispersible micelles when $pH > pK_a$ (Cistola et al., 1988). Despite no structural analysis of the lipidic samples were performed in this work, these earlier findings correlate with the interpretation of the current results, i.e. that aggregates that are released into the aqueous phase are generated at pH 10 but not at pH 6 (oleic acid $pK_a \sim 7.5$, see Fig. 8).

For simplicity, the current presentation considers the fatty acids as simple titratable molecules which solely interact by repulsive charge–charge interactions via the carboxylic groups. Other interactions are of course possible between the lipid molecules in the film (i.e. among triacylglycerols, lysoacylglycerols and free fatty acids). Thus, an equilibrium between molecular attraction and repulsion between these lipidic molecules within the film must exist, which includes both electrostatic repulsive forces and attractive forces such as hydrogen bonding networks, van der Waals forces (dispersion forces), and hydrophobic interactions. However, since the interpretation of the current data correlate with the simple view of fatty acids with charge–charge interactions only, these electrostatic repulsive interaction forces are presumably overpowering the attractive forces.

## 5. Conclusion

The combined use of ATR-FTIR, QCM-D, and TIRF have elucidated some highly interesting details about the mechanisms of lipase adsorption and activity on a surface supported triacylglycerol film, as well as the removal of triacylglycerol digests from the surface. It was found that in a sequential pH system, where hydrolysis was performed at pH 6 followed by a rinse at pH 10, the total lipid removal is significantly enhanced compared to the reaction performed constantly at pH 10. It was also found that lipase adsorption is larger at pH 6 than at pH 10, and that desorption of adsorbed lipase at pH 6 occurs when shifting to pH 10. It is proposed that the main reason for these observations is based in the electrostatic repulsion between negative potentials within the lipid film as well as between the lipid film and lipase protein surface.

## Acknowledgements

The authors are grateful to Dr. Kim Borch, Dr. Claus C. Fuglsang, and Dr. S.A. Patkar (Novozymes, Denmark) for fruitful discussions and for the supply of highly purified lipases. MTNP acknowledges the support from the Danish Research Council (Innovation Post Doc program), Novozymes, and Novo-Nordisk.

## References

Aaslyng, D., Gormsen, E., Malmos, H., 1991. Mechanistic study of proteases and lipases for the detergent industry. J. Chem. Tech. Biotechnol. 50, 321–330.

Buijs, J., Hlady, V., 1997. Adsorption kinetics, conformation, and mobility of the growth hormone and lysozyme on solid surfaces, studied with TIRF. J. Colloid Interface Sci. 190, 171–181.

Cistola, D.P., Hamilton, J.A., Jackson, D., Small, D.M., 1988. Ionization and phase behaviour of fatty acids in water: application of the Gibbs phase rule. Biochemistry 27, 1881–1888.

Dambmann, C., Holm, P., Jensen, V., Nielsen, M.H., 1971. How enzymes got into detergents. Dev. Ind. Microbiol. 12, 11–23.

Fujii, T., Tatara, T., Minagawa, M., 1986. Studies on application of lipolytic enzyme in detergency I. J. Am. Oil Chem. Soc. 63, 796–799.

Flipsen, J.A.C., Appel, A.C.M., van der Hijden, H.T.W.M., Verrips, C.T., 1998. Mechanism of removal of immobilized triacylglycerol by lipolytic enzymes in a sequential laundry wash process. Enzyme Microb. Technol. 23, 274–280.

Fojan, P., Jonson, P.H., Petersen, M.T.N., Petersen, S.B., 2000. What distinguishes a lipase from an esterase: a new practical approach. Biochimie 82, 1033–1041.

Griffiths, P.R., de Haseth, J.A., 1986. Fourier Transform Infrared Spectroscopy. John Wiley & Sons Inc (ISBN 0-471-09902-3).

Harrick, N.J., 1967. Internal Reflection Spectroscopy. Harrick Scientific Corporation (ISBN 0-933946-13-9).

Höök, F., Rodahl, M., Keller, C., Glasmäster, K., Frederiksson, C., Dahlqvist, P., Kasemo, B., 1999. The dissipative QCM-D Technique: interfacial phenomena and sensor applications for proteins, biomembranes, living cells and polymers. In: Proceedings of Joint Meeting of The European Frequency and Time Forum and The IEEE International Frequency Control Symposium, vol. 2, pp. 966–972.

Höök, F., Kasemo, B., Nylander, T., Fant, C., Sott, K., Elwing, H., 2001. Variations in coupled water, viscoelastic properties, and film thickness of a Mefp-1 protein film during adsorption and cross-linking: a quartz crystal microbalance with dissipation monitoring, ellipsometry, and surface plasmon resonance study. Anal. Chem. 73, 5796–5804.

Marinova, K.G., Alargova, R.G., Denkov, N.D., Velev, O.D., Petsev, D.N., Ivanov, I.B., Borwankar, R.P., 1996. Charging of oil–water interfaces due to spontaneous adsorption of hydroxyl ions. Langmuir 12, 2045–2051.

Neves-Petersen, M.T., Fojan, P., Petersen, S.B., 2001a. How do lipases and esterases work: the electrostatic contribution. J. Biotechnol. 85, 115–147.

Neves-Petersen, M.T., Petersen, E., Fojan, P., Noronha, M., Madsen, R.G., Petersen, S.B., 2001b. Engineering the pH-optimum of a triglyceride lipase: from predictions based on electrostatic computations to experimental results. J. Biotechnol. 87, 225–254.

Neves-Petersen, M.T., Petersen, S.B., 2003. Protein electrostatics: a review of the equations and methods used to model electrostatic interactions in biomolecules—applications in Biotechnology. Biotechnol. Annu. Rev. 9, 315–395.

Petersen, S.B., Jonson, P.H., Fojan, P., Petersen, E.I., Neves-Petersen, M.T., Hansen, S., Ishak, R.J., Hough, E., 1998. Protein engineering the surface of enzymes. J. Biotechnol. 66, 11–26.

Rodahl, M., Höök, F., Fredriksson, C., Keller, C.A., Krozer, A., Brzezinski, P., Voinova, M., Kasemo, B., 1997. Simultaneous frequency and dissipation factor QCM measurements of biomolecular adsorption and cell adhesion. Faraday Discuss. 107, 229–246.

Small, D., 1986. Lipid Res. 4, 285.

Snabe, T., Petersen, S.B., 2002. Application of infrared spectroscopy (attenuated total reflection) for monitoring enzymatic activity on substrate films. J. Biotechnol. 95, 145–155.

Snabe, T., Petersen, S.B., 2003. Lag phase and hydrolysis mechanisms of triacylglycerol film lipolysis. Chem. Phys. Lipids 125, 69–82.

Voinova, M.V., Rodahl, M., Jonson, M., Kasemo, B., 1999. Viscoelastic acoustic response of layered polymer films at fluid–solid interfaces: continuum mechanics approach. Physica Scripta 59, 391–399.